Green Chemistry

PAPER

View Article Online
View Journal | View Issue

Cite this: *Green Chem.*, 2024, **26**, 8341

Nickel-catalyzed cross-coupling aminations *via* high-throughput mechanochemistry enabled by resonant acoustic mixing†

Alice Nanni, [a] Deshen Kong,[a] Chen Zhu [a,b] and Magnus Rueping *[a]

Received 11th April 2024,
Accepted 13th June 2024

DOI: 10.1039/d4gc01790k

rsc.li/greenchem

In recent years, mechanochemistry has become recognized as an efficient, practical, and sustainable alternative for chemical synthesis. Adhering to the principles of green chemistry, mechanochemistry enables solvent-free, faster, and energy-efficient reactions, thereby reducing waste production and enhancing atom economy. Herein, we present a new nickel-catalyzed mechanochemical High Throughput Experimentation (HTE) amination protocol enabled by Resonant Acoustic Mixing (RAM). The developed C–N cross-coupling reactions avoid possible contamination, scaling-up challenges, and parallel reaction limitations by applying an accelerated screening and optimization protocol. The reduced amount of solvents in the reactions and the minimal amount of reagents required highlight the advantages of our approach over most common solvent-based reactions, aligning with the principles of sustainability and resource efficiency. Furthermore, the mechanochemistry methodology demonstrates seamless scalability to a multigram scale without additional optimizations, emphasizing its potential for streamlined, environmentally friendly, and large-scale industrial production.

Introduction

Sustainable catalysis represents a pivotal advancement in chemistry, aligning the pursuit of chemical innovation with environmental responsibility.[1,2] In this context, mechanochemistry offers opportunities to lead the way to a more environmentally benign era in chemistry. In the past few decades, chemical reactions promoted by mechanical processes such as grinding, milling, crushing, and shearing have gained significant recognition in the synthesis of pharmaceuticals and materials due to their economic and environmental advantages.[3–7]

Mechanochemistry provides a way to reduce, or eliminate, the use of solvents from the reaction mixture, allowing syntheses to be conducted independently of the starting materials' solubility.[8] Among these methods, liquid-assisted grinding (LAG) has become a viable alternative to traditional solution-based synthesis. LAG involves the addition of a small quantity of liquid to expedite reactions and facilitate transformations that may not occur with dry grinding alone. This offers access to reactions and products that are difficult to isolate or that have not been accessible before through conventional routes.[9–13] Typically, mechanosynthesis methods employ grinding media, such as balls, to provide mechanical energy to the reaction mixture, thereby accelerating the product formation. However, the presence of grinding agents in the system can sometimes introduce unwanted contamination due to the wear and chipping of the balls or device surfaces, resulting in positive or negative effects.[14] Furthermore, control of the motion of the milling agents across different types of mills is challenging and may lead to difficulties in scaling or require additional adjustment of reaction conditions, including milling frequency, milling time, filling ratio, and the choice and number of milling media.[15,16] Vibration and mixer mill setups are often applied in organic synthesis and involve individual reaction vessels or jars that allow only a small number of reactions to be conducted at a time. This results in long, drawn-out project timelines and may limit the full exploration of reaction scope.

These challenges have driven the scientific community to look up for a rapid, media-free, readily scalable mechanochemical methodology.[17] A Resonant Acoustic Mixer (RAM) is a non-contact, forced-vibrating mixing device that applies a high-intensity acoustic field to achieve highly efficient particle collisions at low frequencies (typically 60 Hz).[18–23] The energy input in a RAM process can be adjusted by altering the acceleration of the oscillating sample container (from 0 to 100*g*),

[a]*KAUST Catalysis Center (KCC) King Abdullah University of Science and Technology (KAUST), Thuwal 23955-6900, Saudi Arabia. E-mail: magnus.rueping@kaust.edu.sa*
[b]*Eastern Institute for Advanced Study, Eastern Institute of Technology, Ningbo, 315200, China*

† Electronic supplementary information (ESI) available. See DOI: https://doi.org/10.1039/d4gc01790k

achieved by modifying the amplitude of its oscillatory motion. This acceleration is typically measured in multiples of the acceleration of gravity, "*g*" (where $g = 9.81\ m\ s^{-2}$). Resonant acoustic mixing is based on the principle of a vertical forced vibrational system that creates micro-mixing zones throughout the entire mixing vessel. This facilitates the movement and homogenization of bulk materials within the vessel, ensuring a uniform energy distribution without the need for external agent interaction.[24]

To date, RAM has been efficiently used to enable metal–organic framework and cocrystal synthesis, mechano-redox catalysis, and coupling reactions.[25–27] Notwithstanding these advancements, mechanosynthesis methodologies can be hindered by various limitations such as challenges in scaling up, and the ability to rapidly screen reaction conditions and broaden the scope, leading to prolonged project timelines. Thus, for an efficient reaction development, the fast screening of reaction parameters in a parallel high-throughput fashion is indispensable.[17] Therefore, high-throughput reaction screening is often being conducted in setups using 96-well plates, which can directly be transferred to the corresponding high-throughput analytical instruments. However, to date, high-throughput mechanochemistry using larger numbers of reactions in parallel, such as the frequently used 96-well plates, has not been applied. Given the features of RAM and its possible advantages, we decided to explore a high-throughput approach that would allow for fast reaction development, optimization, and scope exploration relevant to applications in industrial and academic settings.[18] Here, we describe the first high-throughput mechanochemical catalysis application exemplified by the development of a nickel catalyzed C–N coupling reaction using Resonant Acoustic Mixing (RAM) technology (Fig. 1).

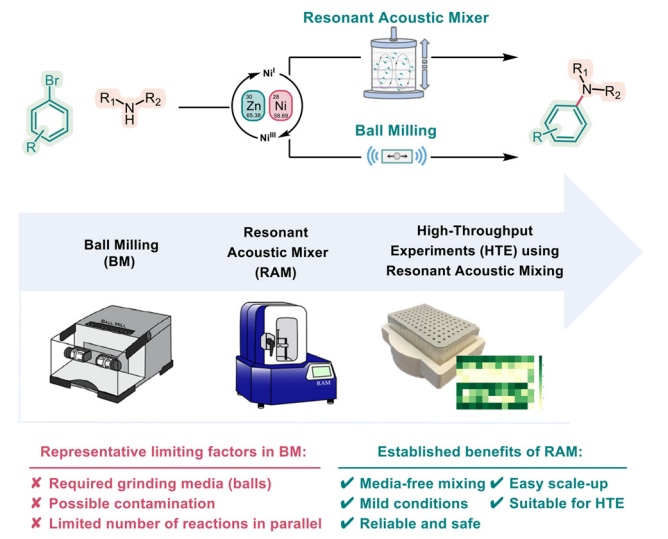

Fig. 1 Mechanochemical strategies for C–N cross-couplings: from ball milling to resonant acoustic mixing enabled high throughput testing and scale-up.

Results and discussion

Given our interest in catalytic C–N bond-forming reactions[28,29] and the high demand for and importance of amines in industry,[30–32] we decided to develop a new mechanochemical amination protocol that utilizes accelerated screening processes through high-throughput experimentation, offering an easy and readily scalable procedure. With the aim of minimizing reaction development time and reducing the amount of reagents required in the screening of reaction conditions, we started with designing, customizing, and 3D printing a 96-well collection plate holder for HTE-RAM for the readily available 1 mL 96-well collection plate (Fig. 2 and the ESI†).

After validating and testing the sample holder setup, a 96-reaction array was used for the development of a mechanochemical Ni-catalyzed C–N bond formation complementing recent work on thermal and piezoelectrical cross-coupling protocols.[33,34] The conditions utilized in this 96-well plate were sourced from the literature on nickel cross-coupling amination,[35–41] as well as our internal knowledge and experience.[29,42,43] Taken together, the initial 96-well plate HTE reaction optimization setup was prepared by testing two amines (piperidine and aniline), three bases (2-*tert*-butyl-1,1,3,3-tetramethylguanidine (BTMG), quinuclidine, and Cs_2CO_3), three metal powders (zinc, magnesium, and manganese), and four liquid-assisted solvents (DMSO, THF, MeCN, and CPME) for the nickel catalyzed cross-coupling amination using 1-(4-bromophenyl)ethan-1-one as the coupling partner and $NiBr_2$dme as a catalyst.

After all reagents were added, the 96-well plate was sealed with a silicone/PTFE cap mat, placed in the resonant mixer, and the reaction was carried out at 100*g* for 90 minutes. Upon completion, the reactions were diluted with ethyl acetate and analyzed using gas chromatography (Fig. 3 and the ESI†). The best reaction conditions with regard to yields and product selectivity were obtained by using zinc as a metal powder, and a small amount of DMSO as a liquid-assisted (LA) solvent. Replacement of zinc powder with other metal powders, mag-

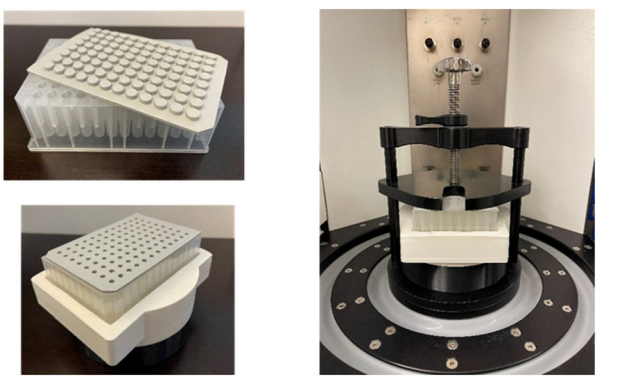

Fig. 2 Readily available 1 mL 96-well plate and sealing (top left), and the 96 well plate in an in-house designed 3D printed holder (bottom left) for application in the RAM system (right).

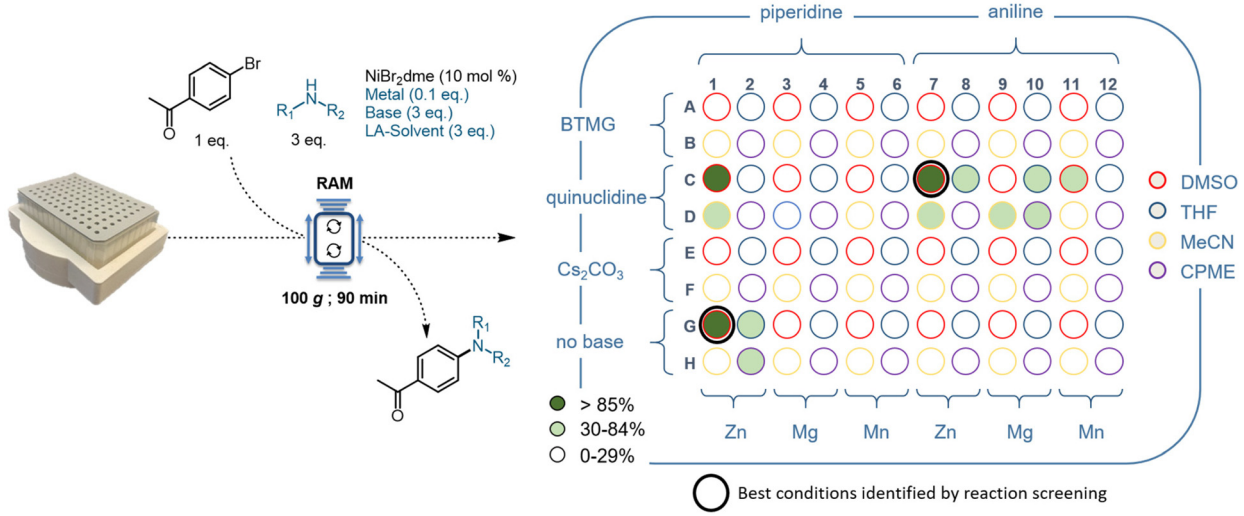

Fig. 3 HTE cross-coupling amination optimization screening. The reaction setup for the nickel-catalyzed cross-coupling included two amines (piperidine and aniline), three bases (BTMG, quinuclidine, and Cs_2CO_3), three metal powders (zinc, magnesium, and manganese), and four liquid-assisted (LA) solvents (DMSO, THF, MeCN, and CPME), using 1-(4-bromophenyl)ethan-1-one as the coupling partner and $NiBr_2$dme as a catalyst. Heatmap visualization generated using GCMS-FID data after min–max normalization. The best reaction conditions for the aliphatic amine are highlighted in black (G1): zinc as a metal powder, DMSO as a liquid-assisted (LA) solvent, and no base. The best reaction conditions for the aromatic amine are highlighted in black (C7): zinc as a metal powder, DMSO as a liquid-assisted (LA) solvent, and quinuclidine as a base.

nesium and manganese, led to lower or no yield (columns 3–6 and 9–12 in Fig. 3). The use of other liquid-assisted solvents, including THF, MeCN, and the green solvent CPME, provided lower or no yields (blue, yellow and purple rings in Fig. 3).

When aromatic amines were used, an external base (quinuclidine) was necessary for the product formation (C7, Fig. 3), whereas no external base was needed for aliphatic amines (G1, Fig. 3), likely due to the basicity and nucleophilicity of the respective amines. The evaluation of different bases showed that both inorganic (Cs_2CO_3) and other organic (BTMG) bases did not furnish the desired product (rows A, B and E, F in Fig. 3).

A series of control experiments confirmed that the nickel catalyst and a sub-stoichiometric amount of reductant are essential for the success of this new protocol (see the ESI†).

Additionally, to strengthen the validity and reliability of our findings, we repeated the 96-well plate HTE optimization reactions, obtaining results consistent with those previously described (see the ESI†).

Encouraged by these results, we decided to explore the substrate scope of the Ni-catalyzed cross-coupling amination using our HTE-RAM setup. As shown in Fig. 4, sterically and electronically diverse aryl bromides were tested in combination with a series of amines containing electron-withdrawing, electron-neutral, and electron-donating groups. The corresponding products were isolated in good yields up to 97%. The transformation exhibits excellent chemoselectivity, as evidenced by its compatibility with various functional groups, including cyano-, ester-, ketone-, sulfone-, trifluoromethyl-, and trifluoromethoxyl groups (**3a–3h**). Notably, *meta*- and *ortho*-substituents are also compatible with the reaction conditions (**3b** and **3d**). To evaluate the possibility of further late-stage functionalization, chloro- and boronic ester containing aryl halides were used, and the corresponding products were obtained in good yields (**3i** and **3j**). The disubstituted aryl bromide (**3k**) also underwent the reaction with good efficiency. Electron-neutral and electron-rich aryl bromides can also be applied in the amination reaction (**3l–3p**). In addition, the reaction also proceeds with good efficiency with bicyclic substrates containing imide, lactone, indanone, quinoline, and benzothiophene motifs (**3q–3u**). Benzamide (**3v**) was also well-tolerated. Additionally, the coupling is compatible with heteroaryl bromides, as demonstrated by the use of pyridine and thiophene (**3w** and **3x**).

Anilines, independently of their electronic nature, can be applied in this protocol. Whereas the use of electron-neutral and electron-rich anilines provided the products in very good yields (**3y–3ac**), significantly weaker nucleophiles such as anilines bearing chloro-, trifluoromethyl-, cyano-, and acetyl groups also afforded the corresponding products albeit in moderate to good yields (**3ad–3af**). Reactions with benzodioxole and sulfane also provided the products with good yields (**3ag** and **3ah**). Furthermore, alkyl-amine nucleophiles were also successful in this protocol. In the presence of indoline, morpholine, and pyrrolidine, the amination products were obtained in good to high yields (**3ai–3ak**). To confirm the reaction's validity, we tested our protocol by coupling a neutral aryl bromide with a neutral amine and an electron-rich aryl bromide with an electron-rich amide; in both cases, the amination products were obtained in good yields (**3al** and **3am**). Primary aliphatic amines were tested in this protocol but failed to yield the desired product due to their lower nucleo-

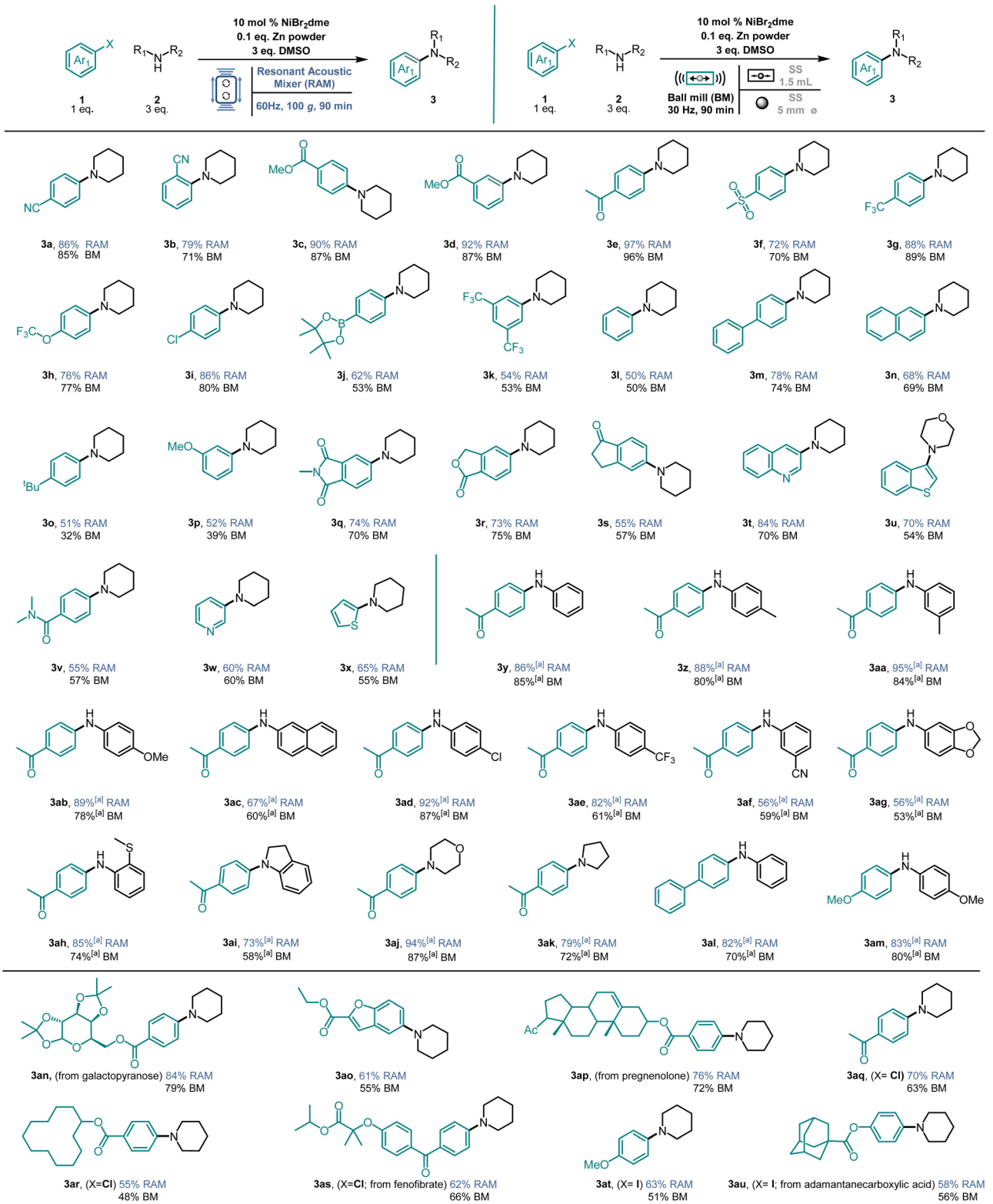

Fig. 4 Scope of substrates. General reaction conditions for resonant acoustic mixing (RAM): aryl halide **1** (0.2 mmol), aniline **2** (0.6 mmol), $NiBr_2$·dme (0.02 mmol), Zn (0.02 mmol), in DMSO (0.8 mmol), 60 Hz for 90 min at 100*g*. General reaction conditions for ball milling (BM): aryl halide **1** (0.2 mmol), aniline **2** (0.6 mmol), $NiBr_2$·dme (0.02 mmol), Zn (0.02 mmol), in DMSO (0.8 mmol), 30 Hz for 90 min. [a]Quinuclidine (0.6 mmol) was used as a base. X═Br, unless specified. Yields after purification.

philicity. Compared to cyclic secondary amines, these substrates are usually less efficient and produce lower yields in nickel-catalyzed cross-coupling reactions.[35,44–46] Secondary acyclic amines were also tested, but no product formation was detected. Additionally, simple and more complex aryl iodides and aryl chlorides can be applied effectively (**3aq** and **3at**), displaying the versatility and validity of this methodology. Notable, biologically relevant, and more complex substrates are also tolerated in this transformation. A series of pharmaceutically relevant heterocyclic substrates, as well as natural-product-derived complex molecules, are all obtained in good yields, showing the potential of this protocol in the functionalization of pharmaceutical-related compounds and bioactive molecules (**3an–3au**).

To further prove the validity of this mechanochemistry protocol, we compared resonant acoustic mixing (RAM) catalysis with ball milling (BM) to understand if the use of balls influences the reaction or if they are needed for the product formation.

All reactions were repeated using an MM400 Mixer mill instrument, using a ∅ 5 mm stainless-steel ball in a 1.5 mL stainless-steel jar, at 30 Hz for 90 minutes. For comparison, the reaction conditions obtained from the 96 well-plate HTE in the RAM were applied. As shown in Fig. 4, reactions with ball milling also reach good to high yields for all the isolated compounds. However, in the majority of cases, the yields are a bit lower compared to the ones achieved using RAM. This indicates that the contact generated by the oscillatory motions of the vessel in the RAM is sufficient to promote reactions between the substrates and the catalyst alone, underscoring the efficacy of RAM in facilitating efficient mixing and reaction kinetics (see the ESI†).

Furthermore, to demonstrate the sustainability and superiority of our method compared to solution-based reactions,[35] we calculated the green metric Process Mass Intensity (PMI).[47] Our method achieved a lower PMI, indicating a more environmentally friendly process with superior environmental benefits (see the ESI†).

Additionally, to highlight the practical utility of this methodology and underscore the effectiveness of RAM, the accelerated Ni cross-coupling amination reaction was tested on a larger scale (Fig. 5).

The reaction of **1e** with **2e** was performed on a 30 mmol scale at 100*g* for 90 min. The desired product **3e** was isolated in a 91% yield (see the ESI†), concordant with the value obtained in the 1 mL 96-well collection plate. Notably, using RAM, no additional optimizations were needed when moving from screening laboratory-scale to multigram-scale reactions, making this technology very promising for fast, efficient, and larger-scale production.

Fig. 5 Multigram-scale nickel-catalyzed amination reactions using the Resonant Acoustic Mixer.

Conclusions

In summary, our study presents a new rapid amination protocol using high-throughput experimentation (HTE). The method is characterized by its mild reaction conditions and minimal solvent usage. RAM enhances C–N cross-coupling reactions without the need for grinding media, thereby mitigating potential issues such as contamination, scale-up challenges, and limitations in conducting parallel reactions. An important feature of RAM is its performance in mechanochemical HTE which facilitates the accelerated screening and optimization of reaction conditions, marking a substantial step forward in efficiency and sustainability. Moreover, the scalability to a multigram scale was demonstrated without the need for additional optimizations, underscoring its potential for streamlined, environmentally friendly, and larger-scale production.

Data availability

The data supporting this article have been included as part of the ESI.†

Conflicts of interest

There are no conflicts to declare.

Acknowledgements

This work was financially supported by the King Abdullah University of Science and Technology (KAUST), Saudi Arabia, Office of Sponsored Research (URF/1/4405 and URF/1/4726).

References

1 J. R. Ludwig and C. S. Schindler, *Chem*, 2017, **2**, 313–316.
2 D. V. Prabhu, *Prog. Chem. Biochem. Res.*, 2022, **1**, 81–89.
3 E. Colacino, A. Porcheddu, C. Charnay and F. Delogu, *React. Chem. Eng.*, 2019, **4**, 1179–1188.
4 P. Ying, J. Yu and W. Su, *Adv. Synth. Catal.*, 2021, **363**, 1246–1271.
5 X. Yang, C. Wu, W. Su and J. Yu, *Eur. J. Org. Chem.*, 2022, e202101440.
6 D. Tan, L. Loots and T. Friščić, *Chem. Commun.*, 2016, **52**, 7760–7781.

7 J. Bonnamour, T.-X. Métro, J. Martinez and F. Lamaty, *Green Chem.*, 2013, **15**, 1116–1120.
8 For representative overviews on mechanochemistry, see: (*a*) M. T. J. Williams, L. C. Morrill and D. L. Browne, *ChemSusChem*, 2022, **15**, e202102157; (*b*) D. Virieux, F. Delogu, A. Procheddu, F. Garcìa and E. Colacino, *J. Org. Chem.*, 2021, **86**, 13885–13894; (*c*) S. Mateti, M. Mathesh, Z. Liu, T. Tao, T. Ramireddy, A. M. Glushenkov, W. Yang and Y. I. Chen, *Chem. Commun.*, 2021, **57**, 1080–1092; (*d*) T. Friščić, C. Mottillo and H. M. Titi, *Angew. Chem., Int. Ed.*, 2020, **59**, 1018–1029; (*e*) A. Porcheddu, E. Colacino, L. de Luca and F. Delogu, *ACS Catal.*, 2020, **10**, 8344–8394; (*f*) M. Pérez-Venegas and E. Juaristi, *ACS Sustainable Chem. Eng.*, 2020, **8**, 8881–8893; (*g*) K. Kubota and H. Ito, *Trends Chem.*, 2020, **2**, 1066–1081; (*h*) I. N. Egorov, S. Santra, D. S. Kopchuk, I. S. Kovalev, G. V. Zyryanov, A. Majee, B. C. Ranu, V. L. Rusinov and O. N. Chupakhin, *Green Chem.*, 2020, **22**, 302–315; (*i*) C. Bolm and J. G. Hernández, *Angew. Chem., Int. Ed.*, 2019, **58**, 3285–3299; (*j*) E. Colacino, A. Porcheddu, C. Charnay and F. Delogu, *React. Chem. Eng.*, 2019, **4**, 1179–1188; (*k*) J. L. Howard, Q. Cao and D. L. Browne, *Chem. Sci.*, 2018, **9**, 3080–3094; (*l*) J. G. Hernández and C. Bolm, *ChemSusChem*, 2018, **11**, 1410–1420; (*m*) D. Tan and T. Friščić, *Eur. J. Org. Chem.*, 2018, 18–33; (*n*) J. G. Hernández and C. Bolm, *J. Org. Chem.*, 2017, **82**, 4007–4019; (*o*) J. L. Do and T. Friščić, *ACS Cent. Sci.*, 2017, **3**, 13–19; (*p*) S. L. James, C. J. Adams, C. Bolm, D. Braga, P. Collier, T. Friščić, F. Grepioni, K. D. M. Harris, G. Hyett, W. Jones, A. Krebs, J. Mack, L. Maini, A. G. Orpen, I. P. Parkin, W. C. Shearouse, J. W. Steed and D. C. Waddell, *Chem. Soc. Rev.*, 2012, **41**, 413–447; (*q*) E. Juaristi and C. G. Avila-Ortiz, *Synthesis*, 2023, 2439–2459; (*r*) Y. S. Zholdassov, L. Yuan, S. R. Garcia, R. W. Kwok, A. Boscoboinik, D. J. Valles, M. Marianski, A. Martini, R. W. Carpick and A. B. Braunschweig, *Science*, 2023, **380**, 1053–1058; (*s*) I. A. A. Silva, E. Bartalucci, C. Bolm and T. Wiegand, *Adv. Mater.*, 2023, **35**, 2304092; (*t*) T. Friščić and W. Jones, *Cryst. Growth Des.*, 2009, **9**, 1621–1637.
9 J. G. Hernández and C. Bolm, *J. Org. Chem.*, 2017, **82**, 4007–4019.
10 K. J. Ardila-Fierro and J. G. Hernández, *ChemSusChem*, 2021, **14**, 2145–2162.
11 W. Pickhardt, S. Grätz and L. Borchardt, *Chem. – Eur. J.*, 2020, **26**, 12903–12911.
12 C. Patel, E. André-Joyaux, J. A. Leitch, X. M. de Irujo-Labalde, F. Ibba, J. Struijs, M. A. Ellwanger, R. Paton, D. L. Browne, G. Pupo, S. Aldridge, M. A. Hayward and V. Gouverneur, *Science*, 2023, **381**, 302–306.
13 C. G. Vogt, S. Gratz, S. Lukin, I. Halasz, M. Etter, J. D. Evans and L. Borchardt, *Angew. Chem., Int. Ed.*, 2019, **58**, 18942–18947.
14 T. Di Nardo and A. Moores, *Beilstein J. Org. Chem.*, 2019, **15**, 1217–1225.
15 N. Fantozzi, J. N. Volle, A. Porcheddu, D. Virieux, F. García and E. Colacino, *Chem. Soc. Rev.*, 2023, **52**, 6680–6714.
16 A. Stolle, R. Schmidt and K. Jacob, *Faraday Discuss.*, 2014, **170**, 267–286.
17 L. Gonnet, C. B. Lennox, J. L. Do, I. Malvestiti, S. G. Koenig, K. Nagapudi and T. Friščić, *Angew. Chem., Int. Ed.*, 2022, **61**, e202115030.
18 K. Nagapudi, E. Y. Umanzor and C. Masui, *Int. J. Pharm.*, 2017, **521**, 337–345.
19 A. A. L. Michalchuk, K. S. Hope, S. R. Kennedy, M. V. Blanco, E. V. Boldyreva and C. R. Pulham, *Chem. Commun.*, 2018, **54**, 4033–4036.
20 H. M. Titi, J. L. Do, A. J. Howarth, K. Nagapudi and T. Friščić, *Chem. Sci.*, 2020, **11**, 7578–7584.
21 F. Effaty, L. Gonnet, S. G. Koenig, K. Nagapudi, X. Ottenwaelder and T. Friščić, *Chem. Commun.*, 2023, **59**, 1010–1013.
22 L. Gonnet, T. H. Borchers, C. B. Lennox, J. Vainauskas, Y. Teoh, H. M. Titi, C. J. Barrett, S. G. Koenig, K. Nagapudi and T. Friščić, *Faraday Discuss.*, 2023, **241**, 128–149.
23 M. Wohlgemuth, S. Schmidt, M. Mayer, W. Pickhardt, S. Grätz and L. Borchardt, *Chem. – Eur. J.*, 2023, e202301714.
24 M. R. Andrews, C. Collet, A. Wolff and C. Hollands, *Propellants, Explos., Pyrotech.*, 2020, **45**, 77–86.
25 J. G. Osorio, E. Hernández, R. J. Romañach and F. J. Muzzio, *Powder Technol.*, 2016, **297**, 349–356.
26 A. Vandenberg and K. Wille, *Constr. Build. Mater.*, 2018, **164**, 716–730.
27 D. H. Leung, D. J. Lamberto, L. Liu, E. Kwong, T. Nelson, T. Rhodes and A. Bak, *Int. J. Pharm.*, 2014, **473**, 10–19.
28 H. Yue, L. Guo, H. H. Liao, C. Zhu and M. Rueping, *Angew. Chem., Int. Ed.*, 2017, **56**, 4282–4285.
29 C. Zhu, H. Yue, J. Jia and M. Rueping, *Angew. Chem., Int. Ed.*, 2021, **60**, 17810–17831.
30 B. R. Brown, *The organic chemistry of aliphatic nitrogen compounds*, Cambridge University, Cambridge, 2004.
31 S. A. Lawrence, *Amines: synthesis, properties and applications*, Cambridge University, Cambridge, 2004.
32 A. Ricci, *Amino group chemistry: from synthesis to the life sciences*, Wiley-VCH, Weinheim, 2008.
33 For selected examples on mechanochemical cross-coupling, see: (*a*) A. C. Jones, W. I. Nicholson, H. R. Smallman and D. L. Browne, *Org. Lett.*, 2020, **22**, 7433–7438; (*b*) Q. Cao, J. L. Howard, E. Wheatley and D. L. Browne, *Angew. Chem., Int. Ed.*, 2018, **57**, 11339–11343; (*c*) J. Yin, R. T. Stark, I. A. Fallis and D. L. Browne, *J. Org. Chem.*, 2020, **85**, 2347–2354; (*d*) D. Kong, D. Ma, P. Wu and C. Bolm, *ACS Sustainable Chem. Eng.*, 2022, **10**, 2863–2867; (*e*) Q. Cao, W. I. Nicholson, A. C. Jones and D. L. Browne, *Org. Biomol. Chem.*, 2019, **17**, 1722–1726; (*f*) K. Kubota, T. Seo, K. Koide, Y. Hasegawa and H. Ito, *Nat. Commun.*, 2019, **10**, 111; (*g*) K. Kubota, T. Endo, M. Uesugi, Y. Hayashi and H. Ito, *ChemSusChem*, 2022, **15**, e202102132; (*h*) T. Seo, N. Toyoshima, K. Kubota and H. Ito, *J. Am. Chem. Soc.*, 2021, **143**, 6165–6175.
34 For selected examples about piezoelectrical reactions in a ball mill, see: (*a*) K. Kubota, Y. Pang, A. Miura and H. Ito,

Science, 2019, **366**, 1500–1504; (*b*) Y. Pang, J. W. Lee, K. Kubota and H. Ito, *Angew. Chem., Int. Ed.*, 2020, **59**, 22570–22576; (*c*) C. Schumacher, J. G. Hernández and C. Bolm, *Angew. Chem., Int. Ed.*, 2020, **59**, 16357–16360; (*d*) Y. M. Wang, Z. W. Zhang, L. C. Deng, T. F. Lao, Z. Q. Su, Y. Yu and H. Cao, *Org. Lett.*, 2021, **23**, 7171–7176; (*e*) H. Lv, X. Xu, J. Li, X. Huang, G. Fang and L. Zheng, *Angew. Chem., Int. Ed.*, 2022, **61**, e202206420; (*f*) M. M. Amer, R. Hommelsheim, C. Schumacher, D. Kong and C. Bolm, *Faraday Discuss.*, 2023, **241**, 79–90; (*g*) T. Seo, K. Kubota and H. Ito, *Angew. Chem., Int. Ed.*, 2023, **62**, e202311531; (*h*) X. Wang, X. Zhang, L. Xue, Q. Wang, F. You, L. Dai, J. Wu, S. Kramer and Z. Lian, *Angew. Chem., Int. Ed.*, 2023, **62**, e202307054.

35 R. Sun, Y. Qin and D. G. Nocera, *Angew. Chem., Int. Ed.*, 2020, **59**, 9527–9533.

36 A. C. Jones, W. I. Nicholson, J. A. Leitch and D. L. Browne, *Org. Lett.*, 2021, **23**, 6337–6341.

37 J. Bariwal and E. Van der Eycken, *Chem. Soc. Rev.*, 2013, **42**, 9283–9303.

38 D. Han, S. Li, S. Xia, M. Su and J. Jin, *Chem. – Eur. J.*, 2020, **26**, 12349–12354.

39 E. B. Corcoran, M. T. Pirnot, S. Lin, S. D. Dreher, D. A. DiRocco, I. W. Davies, S. L. Buchwald and D. W. C. MacMillan, *Science*, 2016, **353**, 279–283.

40 M. S. Oderinde, N. H. Jones, A. Juneau, M. Frenette, B. Aquila, S. Tentarelli, D. W. Robbins and J. W. Johannes, *Angew. Chem., Int. Ed.*, 2016, **55**, 13219–13223.

41 M. O. Konev, T. A. McTeague and J. W. Johannes, *ACS Catal.*, 2018, **8**, 9120–9124.

42 C. Zhu, A. P. Kale, H. Yue and M. Rueping, *JACS Au*, 2021, **1**, 1057–1065.

43 A. Sagadevan, A. Ghosh, P. Maity, O. F. Mohammed, O. M. Bakr and M. Rueping, *J. Am. Chem. Soc.*, 2022, **144**, 12052–12061.

44 C.-H. Lim, M. Kudisch, B. Liu and G. M. Miyake, *J. Am. Chem. Soc.*, 2018, **140**(24), 7667–7673.

45 M. Kudisch, C.-H. Lim, P. Thordarson and G. M. Miyake, *J. Am. Chem. Soc.*, 2019, **141**(49), 19479–19486.

46 C. Rosso, S. Gisbertz, J. D. Williams, H. P. L. Gemoets, W. Debrouwer, B. Pieber and C. O. Kappe, *React. Chem. Eng.*, 2020, **5**, 597–604.

47 N. Fantozzi, J.-N. Volle, A. Porcheddu, D. Virieux, F. Garcıa and E. Colacino, *Chem. Soc. Rev.*, 2023, **52**, 6680.